AAC
Journals.ASM.org

A PBP 2 Mutant Devoid of the Transpeptidase Domain Abolishes Spermine–β-Lactam Synergy in *Staphylococcus aureus* Mu50

Xiangyu Yao[a] and Chung-Dar Lu[a,b]

Department of Biology, Georgia State University, Atlanta, Georgia, USA,[a] and Department of Medical Laboratory Sciences and Biotechnology, China Medical University, Taichung, Taiwan[b]

Exogenous spermine was reported to enhance the killing of methicillin-resistant *Staphylococcus aureus* (MRSA) by β-lactams through a strong synergistic effect of unknown nature. Spermine alone also exerts an antimicrobial activity against *S. aureus* in a pH-dependent manner. MIC measurements revealed stronger effects of spermine under alkaline conditions, suggesting the nucleophilic property of spermine instead of its positive charge as the cause of adverse effects. A spontaneous suppressor mutant (MuM) of MRSA Mu50 was selected for spermine resistance and conferred complete abolishment of spermine–β-lactam synergy. In comparison to that in Mu50, the spermine MIC in MuM remained constant (64 mM) at pH 6 to 8; however, MuM, a heat-sensitive mutant, also grew in a very narrow pH range. Furthermore, MuM acquired a unique phenotype of vancomycin-spermine synergy. Genome resequencing revealed a 7-bp deletion in *pbpB*, which results in a truncated penicillin-binding protein 2 (PBP 2) without the transpeptidase domain at the C terminus while the N-terminal transglycosidase domain remains intact. The results of fluorescent Bocillin labeling experiments confirmed the presence of this defective PBP 2 in MuM. All the aforementioned phenotypes of MuM were reverted to those of Mu50 after complementation by the wild-type *pbpB* carried on a recombinant plasmid. The anticipated changes in cell wall metabolism and composition in MuM were evidenced by observations that the cell wall of MuM was more susceptible to enzyme hydrolysis and that MuM exhibited a lower level of autolytic activities. Pleiotropic alterations in gene expression were revealed by microarray analysis, suggesting a remarkable flexibility of MuM to circumvent cell wall damage by triggering adaptations that are complex but completely different from that of the cell wall stress stimulon. In summary, these results reveal phenotypic changes and transcriptome adaptations in a unique *pbpB* mutant and provide evidence to support the idea that exogenous spermine may perturb normal cell wall formation through its interactions with PBP 2.

Methicillin-resistant *Staphylococcus aureus* (MRSA) constitutes a major health concern due to its numerous mechanisms of virulence and rapid acquisition of genes conferring resistance to β-lactams. New agents that can suppress or abrogate the emergence of resistance, therefore, are in great demand. Here we are interested in the potential application of biogenic polyamines, a group of small polycationic compounds widely distributed in prokaryotic and eukaryotic cells (8), to enhancing the bacterial susceptibility to β-lactam antibiotics. While spermine (a tetraamine) at high concentrations was reported to exert an intrinsic antibacterial activity in *S. aureus* (12), our previous studies have demonstrated the capability of exogenous spermine at low concentrations to reverse MRSA susceptibility to β-lactams (20). However, the molecular mechanism of this strong synergistic effect by spermine and β-lactams in *S. aureus* was still unclear.

β-Lactam antibiotics function by irreversibly occupying the serine residue at the active sites of penicillin-binding proteins (PBPs), and formation of this stable ester-linked acyl enzyme inhibits the transpeptidation step during cell wall cross-linking (11). In *S. aureus*, there are four native PBPs (PBPs 1 to 4) and one acquired PBP, PBP 2a, which is characteristic of MRSA. In contrast to other PBPs, PBP 2a, encoded by the *mecA* gene, shows low affinity to β-lactams due to inefficient formation of the acyl-PBP intermediate and thus ensures continued cell wall synthesis when normal PBPs are inactivated by β-lactams (13). Besides *mecA*, additional factors affecting cell wall architecture or synthesis are believed to have the potential to perturb or modulate β-lactam resistance in *S. aureus*, such as glycan chain length (27), stem peptide configuration (10), pentaglycine cross-bridges (3), and coordinated activity of peptidoglycan (PG) biosynthesis and autolysis (2). Particularly, one of the native PBPs, PBP 2, is essential for the high level of methicillin resistance in MRSA. PBP 2 belongs to the high-molecular-weight class A PBPs, with a transglycosidase (TG) domain and a transpeptidase (TP) domain. When exposed to β-lactams, PG synthesis in MRSA can be achieved at the division septum, mediated by the cooperative functioning of the TG domain of PBP 2 and the TP domain of PBP 2A, possibly as part of a multienzyme complex in cell wall synthesis (27, 29).

In the current study, we isolated an MRSA strain derivative (MuM) conferring spermine resistance by serial passages *in vitro* and compared its genetic basis as well as its phenotypic profiles with those of its parental strain Mu50. We found that this mutant not only shows a 32-fold increase in tolerance of growth inhibition by spermine but also has completely lost the spermine–β-lactam synergy. Furthermore, a 7-bp deletion within the *pbpB* gene, which encodes the essential PBP 2, was revealed by genome resequencing, through which the transpeptidase activity was deprived. Complementation of plasmid-borne wild-type *pbpB* to the mu-

Received 29 July 2011 Returned for modification 26 September 2011
Accepted 9 October 2011
Published ahead of print 17 October 2011
Address correspondence to Chung-Dar Lu, biocdl@gsu.edu.
Supplemental material for this article may be found at http://aac.asm.org/.

doi:10.1128/AAC.05415-11

tant can restore its sensitivity to both spermine and the synergy. In addition, reduced tolerance of the cell wall to hydrolysis and decreased autolytic activity were observed in this mutant, which may be due to changes in cell wall metabolism as a result of this *pbpB* lesion. This mutation also had a pleiotropic effect on gene expression as revealed by transcriptome analysis. Taken together, our results lend support to the idea that exogenous spermine may affect cell wall synthesis through its interactions with PBP 2 and/or PBP 2-assoicated multienzyme machineries to enhance the killing effects of β-lactam antibiotics.

MATERIALS AND METHODS

Bacterial strains, plasmids, and growth conditions. *S. aureus* Mu50 (ATCC 700699), COL (obtained from NARSA), and RN4220 (kindly provided by R. P. Novick) and *Escherichia coli* DH5α (Bethesda Research Laboratories) were employed in this study. Plasmid pCN38 (carrying ampicillin and chloramphenicol resistance), a shuttle vector of *E. coli* and *S. aureus* (6), was used for gene cloning. Both *E. coli* and *S. aureus* strains were routinely grown and maintained in the Luria-Bertani (LB) medium. When required, the LB medium was buffered with 20 mM Tris-HCl at the indicated pH. Antibiotics were added to the medium as necessary at the following concentrations: ampicillin, 100 μg/ml (for *E. coli*); chloramphenicol, 10 μg/ml (for *S. aureus*).

Isolation of spermine-resistant mutants. Spontaneous mutants of MRSA Mu50 (oxacillin MIC of 512 μg/ml and spermine MIC of 1 mM at pH 8.0) were isolated by spreading 1×10^8 CFU of log-phase cells onto spermine-containing plates (2 to 8 mM, pH 8.0) and incubated overnight at 37°C. One independent colony was recovered from plates with 8 mM spermine, and it remained resistant to spermine (up to 32 mM) in broth and on plates. This mutant strain was designated MuM in this study.

Genotypic characterization of spermine-resistant mutant MuM. The chromosomal mutation in MuM was identified by pyrosequencing carried out using the 454 Life Sciences Technology at the University of Florida. Genomic DNAs from both Mu50 and MuM were sent for sequencing, assembled, and compared to the published genomic sequence of *S. aureus* Mu50 (GenBank accession no. BA000017.4). The mutation unique to MuM identified in the *pbpB* gene was confirmed by PCR amplification and DNA sequencing with primers 5′-GGT TTA GTT GCT ATA TCT GGT GG-3′ and 5′-CGC GTT GTT ATA AGT ACC ACC G-3′.

Spermine and antibiotic susceptibility tests. MICs of antibiotics or spermine were determined by a liquid microdilution method according to the guidelines of the Clinical and Laboratory Standards Institute (7). Serial 2-fold dilutions of tested compounds were prepared in a 96-well microtiter tray, and fresh overnight cultures of each bacterial strain were diluted and inoculated with approximate 10^5 CFU/well. Cells were incubated without shaking at 37°C for 24 h (or for up to 36 h as specified). The lowest concentration of antimicrobial agent at which cells were not able to grow was defined as its MIC.

Transcriptome analysis. Mu50 and MuM were grown in Tris-buffered LB (pH 7.5), and cultures in the exponential phase (optical density at 600 nm [OD_{600}] of around 1.0) were immediately treated with the RNA protection reagent (Qiagen) before harvesting. RNA samples were extracted from cells with phenol (Fisher), digested with RNase-free DNase I (Roche) to remove genomic DNA, and purified with RNeasy minicolumns (Qiagen). cDNA synthesis, fragmentation, and terminal labeling were carried out according to the protocols of the manufacturer (Affymetrix). Labeled cDNA was hybridized to the GeneChip *S. aureus* genome array. After scanning, the images were processed with GCOS 1.4 software (Affymetrix). Data from three independent biological experiments were analyzed by comparing gene expression by MuM to that by Mu50, with a fold change of over 2.5 and signal intensity value of 200 as the threshold.

Complementation of *pbpB*. The *pbpB* gene was reported to be transcribed independently or as a polycistronic RNA from its upstream *prfA* promoter (28). To ensure optimal expression, a 3.2-kb fragment covering both *prfA* and *pbpB* was amplified by PCR from the Mu50 genomic DNA with the primers 5′-CGC GGA TCC ACA CAT ACT TGT ACT TGC CTC-3′ (forward and 5′-CGC GGC GCC GAG TGG ATT AGT TGA ATA TAC CTG TTA ATC CAC CGC TG-3′ (reverse). The resulting PCR product was cloned into the BamHI and NarI sites of the shuttle vector pCN38. The recombinant plasmid pYX9 was first cloned into and extracted from *E. coli* and then electroporated into *S. aureus* RN4220 (Bio-Rad Gene-Pulser Xcell) with parameters as described previously (19). Plasmid DNA isolated from recombinant strains of RN4220 was subsequently introduced into Mu50 and MuM by electroporation.

PBP profiling. Membrane fractions were prepared as described previously (25) for detection of PBPs. Protein samples (50 μg) were incubated with 5 μM Bocillin FL (Invitrogen) for 30 min, followed by SDS-PAGE on a 10% gel. The fluorescent Bocillin covalently bound to the PBPs was detected with excitation at 488 nm and emission at 520 nm (Typhoon 9400). Due to its low affinity to Bocillin, PBP 2a was detected by immunoblotting with mouse anti-PBP 2a antibodies (Abnova; 1:5,000 dilution), followed by rabbit anti-mouse IgG antibodies conjugated with alkaline phosphatase (Sigma; 1:30,000 dilution) and chromogenic substrates.

Triton X-100-induced autolysis assays. The Triton X-100-induced autolysis assay was conducted by following a protocol as described previously (9) with minor modifications. Briefly, cells were harvested, washed twice with ice-cold water, and then resuspended in the same volume of 50 mM Tris-HCl (pH 7.2) containing 0.05% Triton X-100. Cells were incubated at 30°C with shaking (~250 rpm) and checked for lysis by measuring the progressive decrease in absorbance (OD_{600}). Autolysis was quantified as a percentage of the initial OD_{600} remaining at each sampling point.

Preparation of autolytic enzyme extracts. Cellular extracts enriched with autolytic enzymes were prepared as previously described (16) with some modifications. Briefly, the cells were grown to mid-exponential phase in 20 ml of LB (20 mM Tris-Cl, pH 7.5) at 37°C with aeration to an OD_{600} of 1, chilled on ice, harvested by centrifugation, and washed twice with ice-cold 50 mM Tris-HCl (pH 7.5) buffer with 150 mM NaCl. The pellet was directly suspended in 80 μl of 4% SDS for 30 min at room temperature or in 400 μl of a solution containing 3 M LiCl and 0.1% Triton X-100 for 30 min at 4°C with stirring. After centrifugation at 10,000 × *g* for 10 min, the supernatants were collected as SDS extracts or LiCl extracts, which were used in zymographic analysis or *in vitro* enzymatic hydrolysis of crude cell walls, respectively.

Enzymatic hydrolysis of crude cell walls *in vitro*. Enzymatic hydrolysis of crude cell walls *in vitro* was performed as previously described (2). Briefly, crude cell walls were prepared from cells (10 ml) grown to mid-exponential phase (OD_{600} of around 1). Cell pellets were boiled in 8% SDS for 30 min and washed three times with hot water to remove SDS. The obtained pellets, as crude cell walls, were suspended in 50 mM Tris-HCl (pH 7.5) to an OD_{600} of 0.6, and LiCl extracts as described above were added to start hydrolysis. The reaction was conducted at 37°C with shaking (~250 rpm), and the hydrolysis rate was measured as a decrease of OD_{600}.

Zymographic analysis. Heat-killed cells of *S. aureus* RN4220 were prepared as the substrate for hydrolytic enzymes. Briefly, cells in mid-exponential phase were harvested, and the pellet was suspended in 2× Laemmli SDS sample buffer and heated for 5 min at 100°C. The heat-inactivated cells (with an OD_{600} equivalent to 10) in 1/10 volume of the resolving-gel (10%) solution was added to cast the gel, and the SDS extracts as described above were subjected to this SDS-PAGE to detect the hydrolytic activities. After electrophoresis, the gel was soaked for 30 min in distilled water at room temperature and then transferred into the renaturing buffer (25 mM Tris-HCl, 1% [vol/vol] Triton X-100, pH 8.0) with gentle shaking for 16 h at 37°C to allow for renaturation. The renatured autolysins appear as clear translucent bands on the opaque background, and the contrast can be enhanced for photography by staining the gels in 1% (wt/vol) methylene blue with 0.05% KOH.

Preparation and analysis of extracellular protein fraction. For the preparation of extracellular protein extracts, bacteria were grown in LB

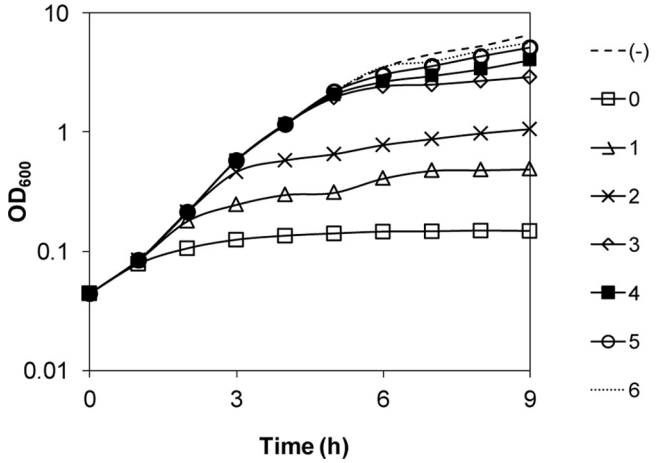

FIG 1 Growth inhibition by exogenous spermine. Cells from a fresh overnight seed culture were inoculated into prewarmed LB broth (pH 8.0). Spermine (10 mM) was added at the indicated time points after inoculation, and OD_{600} was monitored at 1-h intervals.

medium to exponential phase. After centrifugation, extracellular proteins in the supernatant (2 ml) were precipitated with 0.02% sodium deoxycholate at 4°C for 30 min followed by 10% (wt/vol) trichloroacetic acid at −20°C overnight. The precipitates were harvested by centrifugation at 4°C and 16,000 × *g* for 20 min, washed with 100% ice-cold acetone twice, and dried. The protein pellets were resolved in an appropriate volume of Laemmli SDS sample buffer, boiled, and separated by 10% SDS-PAGE. Bands showing different intensities in MuM and Mu50 samples were identified by matrix-assisted laser desorption ionization–time of flight tandem mass spectrometry (MALDI-TOF MS-MS).

ESI-MS. Solutions of spermine and oxacillin (2 mM), either alone or in combination, were prepared in ammonium acetate buffer (5 mM), and the final pH was adjusted with formic acid or ammonium hydroxide. All solutions were directly injected for electrospray ionization mass spectrometry (ESI-MS) analysis. Mass spectral acquisition was done in the positive-ion mode using the following parameters: capillary voltage, 3,000 V; sample cone voltage, 35 V; extraction cone voltage, 2.5 V; source temperature, 120°C; desolvation temperature, 150°C; gas flows desolvation, 500 liters/h; and pump flow rate, 5 μl/min.

RESULTS

Growth inhibition of Mu50 by spermine is pH dependent. While spermine and β-lactams exert a strong synergy effect on MRSA (20), spermine alone can cause growth inhibition of all tested strains of *S. aureus* (Mu50, N315, COL, and RN4220, with MICs of 1 mM, 1 mM, 0.5 mM, and 2 mM, respectively, at pH 8.0). To further understand the adverse effect of spermine, we first tested whether this effect is growth phase dependent. As shown in Fig. 1, growth of Mu50 in the buffered LB broth (20 mM Tris-Cl, pH 8.0) was immediately inhibited by the addition of spermine (10× MIC; 10 mM) regardless of the growth stage.

Spermine is a tetra-amine, and its four pK_a values were reported as 10.86, 10.05, 8.82, and 7.95 (4). At pH 7.4, the relative abundance of +4/+3 species was 3/1, and the ratio could be 1/1 at pH 8.0. If not protonated, the amino group would serve as a nucleophile for potential chemical reactions. To analyze the possible effect of spermine net charge on growth inhibition, the spermine MIC was determined for Mu50 suspended in buffered growth media with different pH values, as shown in Fig. 2A. When the pH was at 7.0 or lower, fully positively charged spermine did not have

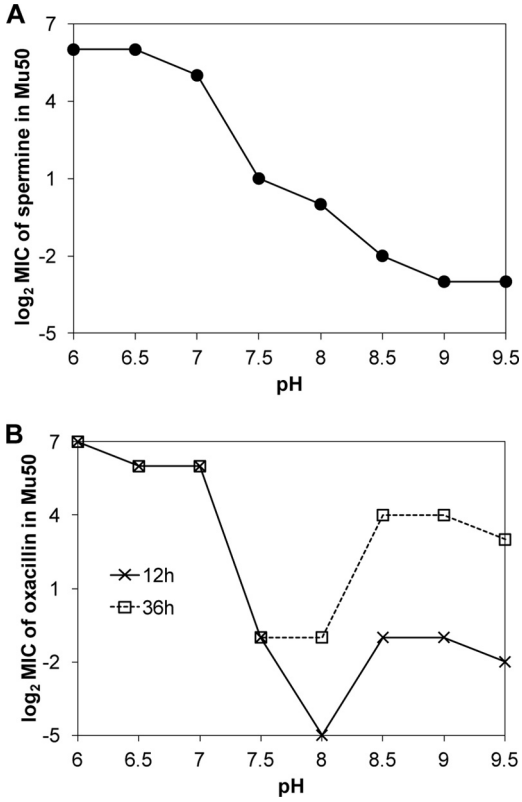

FIG 2 pH-dependent effects of spermine alone (A) or in combination with oxacillin (B). MICs of spermine or oxacillin for Mu50 were determined at different pHs. For measurements of oxacillin MICs, 0.25 times the MIC (for pH 8.0 to 9.5) or 0.5 mM (for pH 6.0 to 7.5) of spermine was included.

a strong inhibitory effect on growth, as reflected by MICs of 32 to 64 mM. Interestingly, the MIC was reduced to 2 mM at pH 7.5 and was decreased further to 0.125 mM at pH 9.0 or higher. Since the net positive charge of spermine is reduced when the pH is increased, these results strongly suggest that the growth inhibition effect of exogenous spermine may not be related to its positive charges and that instead its nucleophilic property may be the cause.

Effects of pH on oxacillin-spermine synergy in Mu50. We also analyzed the pH effect on oxacillin-spermine synergy by measuring the oxacillin MIC in the presence of spermine at different pHs (one-fourth of the MIC for pH 7.5 to 9.5 and 0.5 mM for pH 6 to 7). Like with spermine alone, such synergy also followed the same trend of pH dependence (Fig. 2B) but only when the pH was equal to or lower than 8.0. Unexpectedly, at pH 8.5 and higher, the oxacillin MIC showed the reverse trend and increased 16-fold from that at pH 8.0, and a further 32-fold increment was observed after 24 more hours of incubation. These results led us to propose oxacillin inactivation by a possible chemical reaction between nucleophilic spermine and the β-lactam ring of oxacillin (26).

To test this hypothesis, possible formation of spermine-oxacillin conjugates was analyzed by ESI-MS in the positive-ionization mode, as shown in Fig. 3. In comparison to the mass spectra for spermine and oxacillin (2 mM), a new peak corresponding to the proposed spermine-oxacillin conjugate (*m/z* 604.5) appeared in the mass spectrum of an equimolar mixture (2 mM) of spermine and oxacillin at pH 9.0 but not in that of a

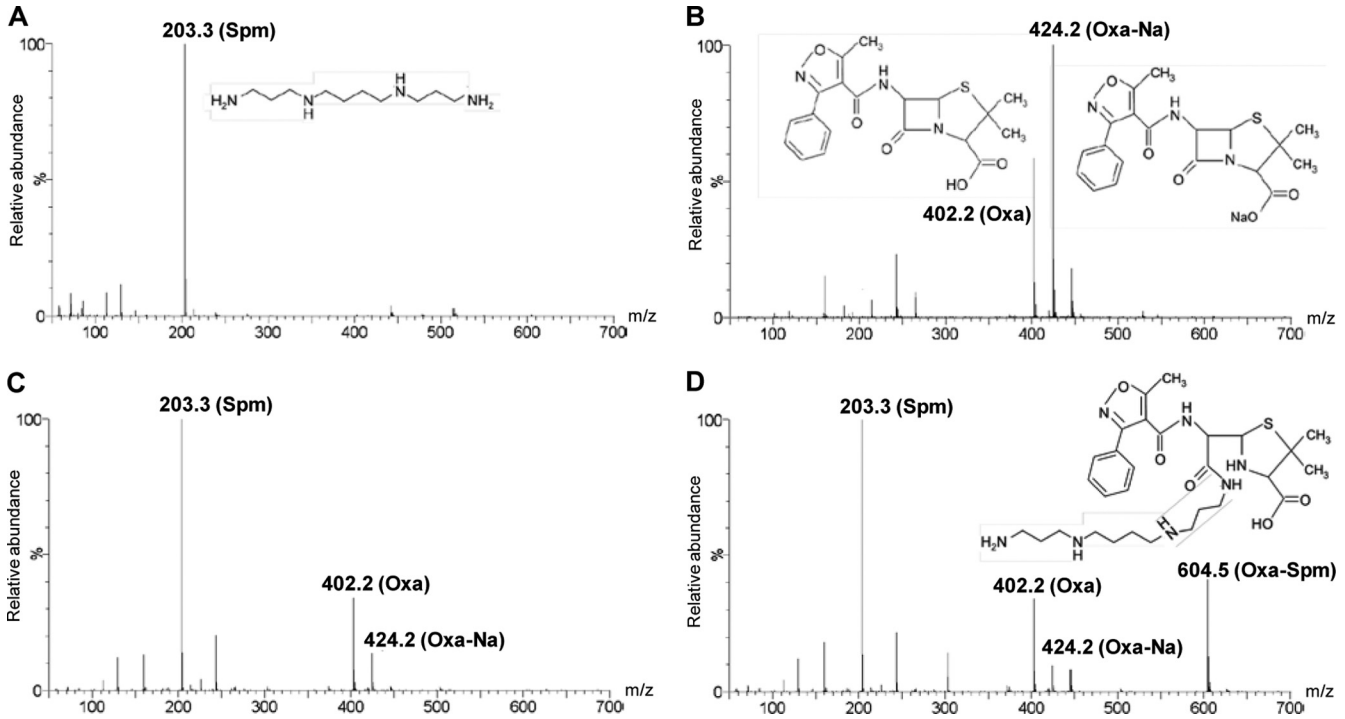

FIG 3 ESI-MS analysis. All compounds were dissolved in ammonium acetate buffer (5 mM), and mass spectra were acquired in positive-ionization mode. (A) Spermine (Spm); (B) oxacillin (Oxa); (C) equimolar mixture of spermine and oxacillin at pH 7; (D) equimolar mixture of spermine and oxacillin at pH 9.

mixture at pH 7.0. These data support pH-dependent formation of chemical conjugates between spermine and β-lactams and are consistent with the patterns of MIC readings in Fig. 2.

Selection and preliminary characterization of a spermine-resistant mutant, MuM. Strain MuM, a spermine-resistant mutant of Mu50, was isolated through selection on high concentrations of spermine as described in Materials and Methods. MuM exhibited resistance to spermine, with an MIC 32-fold higher than that of the parental Mu50 (Table 1). The genetic modification(s) in MuM was specific for spermine, as MICs of several tested antibiotics (streptomycin, tetracycline, gentamicin, erythromycin, chloramphenicol, kanamycin, and spectinomycin) for MuM were the same as those for Mu50. However, we observed significant changes in the growth behavior of MuM. In comparison, colonies of MuM on LB plates were homogeneously smaller than those of the parent strain, and these colonies required over 18 h to recover from the lag phase at 37°C when inoculated into the LB broth. Once in the logarithmic phase, the doubling time of MuM was over 3.5-fold longer than that of Mu50 (127 min versus 35 min) (Fig. 4A). However, fast-growing cells started to appear after continuous passage of MuM on LB plates, suggesting the rise of compensatory mutations from growth impairment (1). To maintain a stable MuM, we found that a glucose supplement in the LB medium was helpful, as evidenced by a reduced doubling time to 70 min with a shortened lag phase (Fig. 4A), and the spermine resistance phenotype as well as homogeneous colony size remained after passages. Another interesting phenotype of MuM was that this strain is a temperature-sensitive mutant; no apparent growth can be detected at 42°C.

Limitation of growth of MuM by pH. To examine the pH dependence of spermine effects on MuM, spermine MICs were measured under conditions of different pH. In contrast to the pH-dependent trend with its parental strain Mu50 (Fig. 2A), the spermine MIC for MuM was estimated to be 64 mM at pH 6.0 to 8.0 but, surprisingly, dropped to an undetectable level at pH 8.5 or higher. This prompted us to monitor the growth of MuM and Mu50 in buffered LB broth of pH 6.0 to 9.5 in the absence of exogenous spermine. Strain Mu50 grew comparably at pH 6.0 to

TABLE 1 MICs of oxacillin, vancomycin, and spermine for Mu50 and MuM

Antibiotic (MIC unit)	MIC[a] for strain: Mu50 Alone	Mu50 With spermine (0.5 mM)	MuM Alone	MuM With spermine (0.5 mM)	Mu50/pYX9 Alone	Mu50/pYX9 With spermine (0.5 mM)	MuM/pYX9 Alone	MuM/pYX9 With spermine (0.5 mM)
Oxacillin (μg/ml)	512	<1	1,024	1,024	512	<1	1,024	<1
Vancomycin (μg/ml)	4	4	2	<0.03	8	4	8	4
Spermine (mM)	2		64		2		2	

[a] MICs were determined in LB broth with the pH adjusted to 7.5. Plasmid pYX9 carries the wild-type *pbpB* gene.

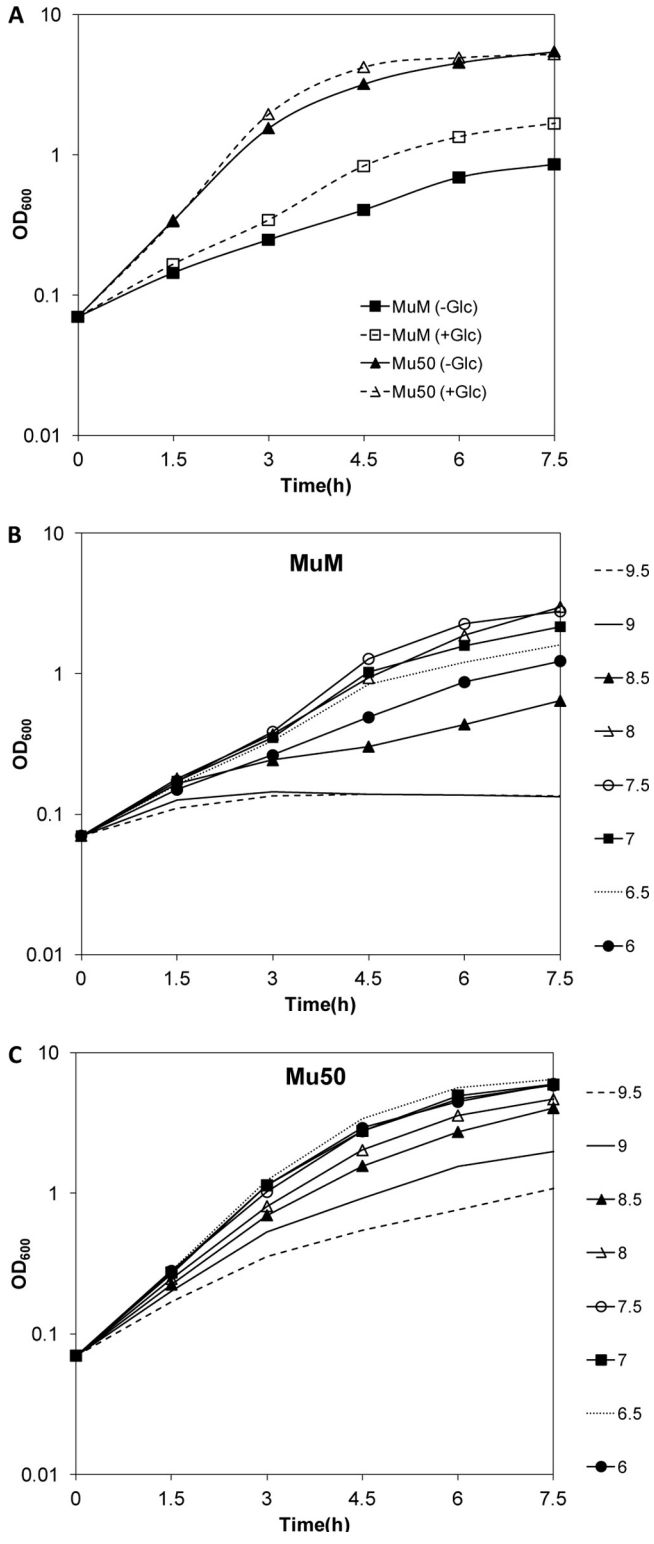

FIG 4 Growth behaviors of Mu50 and MuM. Growth of the cells in LB broth at 37°C with aeration was monitored by OD measurements. (A) Growth in the presence or absence of 0.4% glucose; (B) growth of MuM in LB buffered with 20 mM Tris-HCl at the indicated pH; (C) growth of Mu50 in LB buffered with 20 mM Tris-HCl at the indicated pH.

8.5, and the growth rate was significantly reduced at pH 9 and 9.5 (Fig. 4C). In comparison, MuM exhibited its optimal growth at pH 7.5 to 8.0 and basically showed no growth at pH 9.0 and higher (Fig. 4B).

Loss of spermine–β-lactam synergy and gain of spermine-vancomycin synergy in MuM. MICs of oxacillin and several different types of antibiotics in the presence and absence of spermine were determined for MuM and its parental stain Mu50. The results indicated that while the synergy effect of spermine was exclusively on β-lactams in Mu50, MuM behaved differently from Mu50 only on oxacillin (β-lactams in general) and vancomycin. As shown in Table 1, the MICs of oxacillin in the absence of exogenous spermine were comparable in MuM and Mu50. In the presence of 0.5 mM spermine, over a 500-fold reduction of the oxacillin MIC was observed in Mu50, whereas this sensitization effect was completely compromised in MuM. In the case of vancomycin, while its MIC was not affected by the presence of spermine in Mu50, MuM exhibited a considerable increase of susceptibility to this antibiotic when spermine (0.5 mM) was supplemented (Table 1). As an inhibitor of cell wall synthesis, vancomycin works by binding to the D-Ala-D-Ala moiety, and subsequently blocking cross-linkage, of the murein monomers during the transpeptidation reactions by PBPs (33). Such opposite responses of MuM to β-lactam and vancomycin in the presence of spermine raised the possibility that spermine may directly or indirectly inhibit cell wall synthesis.

Genome resequencing of MuM and Mu50 identifies a genetic defect in *pbpB*. To identify the mutation(s) responsible for spermine resistance, genome resequencing of MuM and Mu50 was conducted with the 454 Sequencer FLX system. On average, total base pair reads exceeded over six times the genome size, and the generated contigs covered more than 98% of the published genome sequence of Mu50. Through sequence comparison, only one sequence variation between Mu50 and MuM was identified: a 7-bp deletion in MuM which was located at nucleotides (nt) 1366 to 1372 within the *pbpB* gene, encoding an essential penicillin-binding protein (PBP) in *S. aureus*, PBP 2 (Fig. 5A). The presence of this deletion in MuM was confirmed by sequencing of a 461-bp fragment covering this region by PCR amplification from the genomic DNAs of Mu50 and MuM.

PBP 2 is composed of 727 amino acids (M_r of 80,236) with an N-terminal transglycosidase domain spanning residues 82 to 258 and a C-terminal transpeptidase domain spanning residues 361 to 629 (Fig. 5A) (UniProtKB/TrEMBL no. Q99U39). All PBPs share a penicillin-binding (PB) domain which binds β-lactam antibiotics due to the structural similarity between β-lactams and the D-Ala-D-Ala moiety of the nascent peptidoglycan, the natural substrate of PBPs. The PB domain is composed of two subdomains, and three motifs broadly conserved in PBPs lie at the interface of these two subdomains. In the case of *S. aureus* PBP 2, these three motifs comprise $SSLK_{401}$, SFN_{456}, and KTG_{585}, with S_{398} being the primary active residue (34). In MuM, a frameshift by the 7-bp deletion in *pbpB* creates an immediate stop codon that truncates the translated product from N_{456}, right at the second consensus motif, and removes the C-terminal transpeptidase domain of PBP 2 (Fig. 5A). As a result, the mutated PBP 2 was expected to lose its formation of an acyl linkage with β-lactams. To test this hypothesis, we conducted PBP labeling with Bocillin, a fluorescent derivative of penicillin. As shown in Fig. 5B, PBP 2 was not detectable in

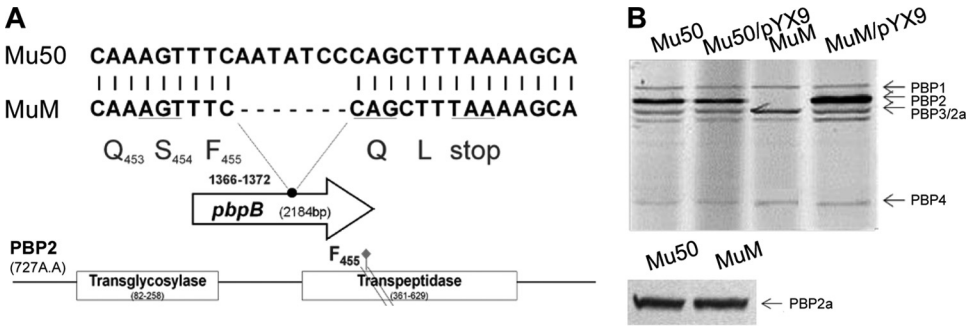

FIG 5 Identification of the *pbpB* lesion in spermine-resistant mutant MuM. (A) Sequence alignment of the *pbpB* genes from Mu50 and MuM at the mutation site. Also shown are the location of the 7-bp deletion (nt 1366 to 1372) in the *pbpB* gene of 2,184 bp, the amino acid sequence of the truncated PBP 2 of MuM, and the sizes and locations of the transglycosidase and transpeptidase domains of PBP 2. (B) The absence of PBP 2 in MuM and the presence of other penicillin-binding proteins were revealed by Bocillin labeling (top panel) or immunoblotting (bottom panel).

the membrane preparation of MuM, supporting the presence of a truncated PBP 2 in this mutant.

Complementation of the spermine-resistant MuM by *pbpB*. Plasmid pYX9 carrying *pbpB* of Mu50 was constructed for complementation tests. As shown in Table 1, in MuM carrying pYX9, spermine sensitivity and the synergy effect of spermine and β-lactams are restored. Plasmid pYX9 also restores the tolerance of MuM to vancomycin to the wild-type level in the presence of spermine. Vector alone (pCN38) does not rescue those phenotypes in MuM (data not shown). MuM/pYX9 grows much faster than MuM, with an estimated generation time comparable to that of Mu50 (data not shown). In addition, the pH sensitivity of growth was diminished in MuM/pYX9, indicating that a correct form of PBP 2 is required for the buildup of a rigid and strong cell wall to resist diverse environmental challenges.

It was suggested that different PBPs may work in concert or form a complex to coordinate PG synthesis (22). In order to see whether the sophisticated regulation of different PBPs can be affected by the addition of PBP 2, PBPs profile in Mu50 and MuM with or without pYX9 were compared. As shown in Fig. 5B, introduction of plasmid-borne wild-type PBP 2 did not have apparent effects on the production of other PBPs. MuM with vector pCN38 alone exhibited the same PBP pattern as observed in MuM (data not shown). Moreover, similar levels of PBP 2a were detected in MuM and Mu50 by immunoblotting (Fig. 5B), suggesting that the genetic lesion of *pbpB* did not affect *mecA* expression in MuM. As described below, we also conducted transcriptome analysis in MuM and Mu50; consistent with the results of Bocillin labeling and PBP 2a immunoblotting, we found comparable levels of expression for all genes encoding penicillin-binding proteins in these two strains (see Table S1 in the supplemental material).

Effects of the truncated PBP 2 in MuM on cell wall hydrolysis. The mutated *pbpB* gene of MuM may result in perturbation of cell wall synthesis and change the PG structure. To test this hypothesis, the sensitivity of MuM and Mu50 cell walls to hydrolytic enzymes was analyzed by incubation with a common source of autolytic enzyme extracts from strain COL. Degradation of the MuM cell wall materials was significantly faster than that for the Mu50 control (Fig. 6A), suggesting that cell walls of MuM may be less cross-linked and/or more susceptible to hydrolysis due to the defects in PBP 2.

It has been reported that enzymes for cell wall synthesis and hydrolysis may be coregulated and that the decreased expression of *pbpB* could repress the autolytic system in *S. aureus* (2). Here a similar situation may occur in the case of MuM. Whole-cell autolysis following exposure of MuM and Mu50 cells to Triton X-100 was assessed. As shown in Fig. 6B, the rate of Mu50 autolysis was significantly higher than that of MuM autolysis. Since the cell wall of MuM was more susceptible to degradation than that of

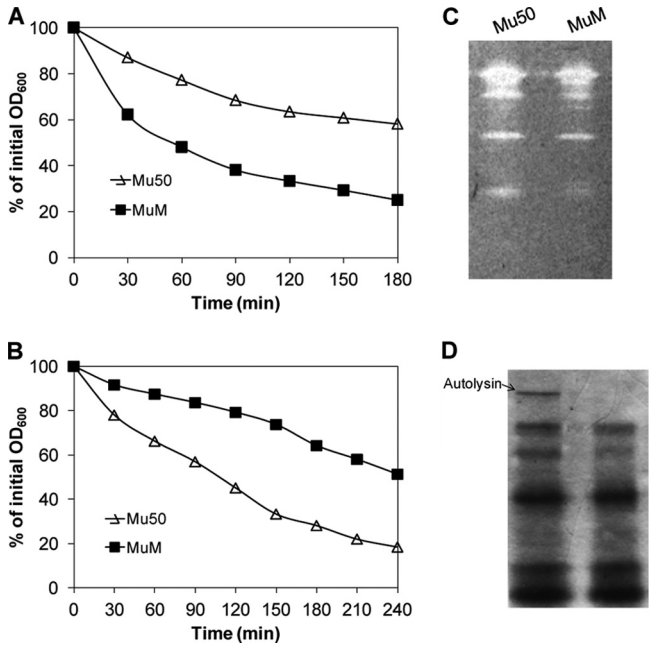

FIG 6 Analysis of cell wall hydrolysis. (A) *In vitro* susceptibility of cell walls. Crude cell walls of Mu50 or MuM were subjected to degradation by autolytic enzymes from *S. aureus* COL. Preparations of these samples are described in Materials and Methods. The experiments were reproduced several times, and data from a single representative experiment are shown. (B) Triton X-100-induced autolysis of Mu50 and MuM cells. Values indicate the average of two independent experiments. (C) Zymographic analysis of the autolysins in SDS cell extracts from Mu50 and MuM. Samples were analyzed in a 10% resolving gel containing heat-killed RN4220 cells. Lytic activity was detected by incubation of the gel with gentle agitation at 37°C in renaturing buffer. Equivalent amounts of protein samples were loaded. (D) Protein profiles in culture supernatants. Extracellular proteins from Mu50 and MuM were prepared as described in Materials and Methods. The gel was stained with Coomassie blue to detect the total secreted protein profile, and the protein band of autolysin was identified by MALDI-TOF MS-MS.

Mu50 (Fig. 6A), the lower rate of autolysis in MuM may be related to a decreased activity and/or quantity of autolytic enzymes, in addition to possible alterations in cell wall composition.

We also conducted zymographic analysis of autolytic enzymes from Mu50 and MuM. With crude cell walls of RN4220 as a substrate, several bacteriolytic bands caused by cell wall hydrolysis by the enzyme extract from MuM were less intense than those from Mu50 (Fig. 6C). Although the exact identities of these affected hydrolytic enzymes cannot be determined from this experiment, they may include the 138-kDa autolysin ATL and its proteolytic products of 62 and 51 kDa (16). In addition, the secreted protein profiles from the spent media of MuM and Mu50 in the logarithmic phase of growth were compared following SDS-PAGE. As shown in Fig. 6D, one polypeptide appeared preferentially in the protein sample of Mu50 but was completely absent in that of MuM, and this peptide was identified as autolysin ATL by MALDI-TOF MS-MS.

While the results in Fig. 6C suggest a reduced activity of cell wall hydrolytic enzymes in MuM, surprisingly, transcriptome analysis (see Table S1 in the supplemental material) revealed no apparent difference between MuM and Mu50 in expression of the major hydrolytic enzymes encoded by *atl*, *sle*, *lytM*, and *SA0620/SAV0665* (2). Since autolysin ATL requires proteolytic processing to reach its maximal activity, these somewhat contradictory results may be explained by a decreased level of ATL proteolytic processing and a greater degree of ATL retention within the cell wall of MuM, perhaps as a consequence of possible alterations in the PG composition due to the *pbpB* lesion.

Transcriptome analysis. The multiple phenotypic changes of MuM prompted us to evaluate the transcriptional profile caused by the defective PBP 2. Logarithmic-phase cells of MuM and Mu50 grown in LB alone without spermine supplement were subjected to transcriptome analysis as described in Materials and Methods. A total of 250 genes showing upregulation and 7 genes showing downregulation in MuM were identified and are listed in Table S1 in the supplemental material. In order to see whether the unique pattern of gene expression in MuM was due to the *pbpB* lesion, we also conducted transcriptome analysis of Mu50 and MuM carrying wild-type *pbpB* in *trans.* When sorted against MuM/pYX9 and Mu50/pYX9 expression profiles, the majority of the changes observed in MuM were greatly attenuated in MuM/pYX9, suggesting that the truncated PBP 2 is responsible for the complicated transcriptional adaptations in MuM. Nonetheless, it is worth noting that there are 10 genes (*czrAB*, *vraDE*, *gntPK*, *oppF*, *mtlF*, *SAV0069*, and *SAV0190*) showing up- or downregulation in MuM regardless of complementation by pYX9, and the fold change of expression of these genes in MuM/pYX9 was even greater than that in MuM.

While one might expect that the *pbpB* lesion of MuM could affect cell wall synthesis and trigger a specific stress response, the gene list in Table S1 in the supplemental material shows no overlap with the reported signature genes of the cell wall stress stimulon (17, 37). Instead, one intriguing observation was the upregulation of 67 genes associated with amino acid biosynthesis and transport that are members of the CodY regulon (23, 32). In *S. aureus*, like in many low-G+C Gram-positive bacteria, CodY is a central regulator mediating amino acid biosynthesis, nitrogen utilization, and transport of macromolecules.

Surprisingly, 67 genes residing in several genomic islands (GIs) were found to be activated in MuM (see Table S1 in the supplemental material), and this list could be expanded further if a less stringent fold change was applied in data analysis. These GIs include SCCmec, IS1181-1, SaPIm2, SaGlm, ϕMu50B, SaPIm3, and ϕMu50A (18). Although little was known about the nature of GI activation, similar activation of GIs was observed in a *murF* conditional mutant (35) in which the cell wall synthesis was perturbed in muropeptide maturation.

Other than the CodY regulon and GIs, genes that were differentially upregulated in MuM were clustered into potential operons: *ureABCEFGD* for urease synthesis, *sbnABCDRFGHI* for iron metabolism, *kdpABCDE* for an inducible potassium uptake system, *SAV2094-thiDME* for vitamin B_2 biosynthesis, and *bioFABD* for vitamin H biosynthesis. Specifically, degradation of urea by urease in *S. aureus* was thought to neutralize acidic microenvironments by generating NH_3 and CO_2 under acid stress (5). In addition, MuM also hosts the induced *arcABCD* operon for the arginine deiminase pathway, a major role of which is to alkalinize the medium by generating NH_3 and CO_2 as well as to energize the cells by production of ATP (36, 39). Together, these findings strongly suggest that MuM is primed to adjust its metabolic activities to increase the internal pH, which would imply that the defective cell wall may alter the membrane potential and somehow exert a mild acid stress on MuM.

DISCUSSION

Unique phenotypic behaviors and transcriptional adaptations of MuM. A spontaneous suppressor mutant of MRSA Mu50 with a mutation conferring resistance to β-lactams in the presence of spermine was isolated through spermine selection. This mutant possesses a unique *pbpB* lesion, in which a 7-bp deletion generates a truncated PBP 2 without the C-terminal transpeptidase (TP) domain while the transglycosidase (TG) domain at the N terminus remains intact. Although this *pbpB* mutant, MuM, still has β-lactam resistance, its physiological properties are very different from those of the parental strain Mu50, a clinical isolate of MRSA, in several aspects: gain of spermine resistance, loss of spermine–β-lactam synergy, gain of spermine-vancomycin synergy, a lower growth rate, a temperature-sensitive growth phenotype, a narrow pH range for growth, changes in cell wall composition and turnover, and a lower level of cell wall hydrolase activity. Furthermore, transcriptome analysis reveals a distinct pattern of gene expression, showing no overlap with that of the cell wall stress stimulon (17, 37).

Physiological functions of PBP 2. Our results indicate that the TP domain of PBP 2 is not essential for growth and β-lactam resistance of MRSA. These conclusions are consistent with a previous report (27) that a Ser_{398}Gly mutation at the TP domain has no effect on the MIC of methicillin but that loss of the TG activity as a result of a Glu_{114}Gln mutation causes a more-than-100-fold decrease in the methicillin MIC. In contrast, the TP activity of PBP 2 is essential for the growth of methicillin-susceptible *S. aureus* (MSSA) (30), and specific mutations at the TP domain (Pro_{458}Leu) can make MSSA resistant to β-lactam antibiotics (22). This discrepancy is due to the presence of a β-lactam-insensitive PBP 2a encoded by the *mecA* gene of MRSA. The TP activity of PBP 2a is able to sustain cell growth when that of PBP 2 is not available. Investigations from that study provide direct evidence that a mutated PBP 2 without the TP activity results in an altered cell wall composition with reduced amounts of highly

cross-linked oligomers. This is consistent with the increased cell wall degradation rate in MuM observed in our study.

In addition to the intrinsic TP and TG activities, PBP 2 may serve as scaffold for a multienzyme complex in cell wall synthesis. The presence of a multienzyme complex in cell wall synthesis was first proposed from studies of *E. coli* (14, 15). Later, Tomasz and coworkers (22, 27) reported evidence to support that PBP 2 forms a complex with PBP 2a, PBP 4, and perhaps other enzymes to coordinate cell wall synthesis and hydrolysis. Along this line, one hypothesis was that the TG and TP activities of PBP 2 are subjected to allosteric regulation within the complex and that the conformation of this complex could be affected by changes in the supporting scaffold of PBP 2. Based upon this model, we propose a working hypothesis for spermine effects on cell wall synthesis in *S. aureus*, as described below. This model may also provide an explanation of a somewhat contradictory report that insertion of a transposon at the 3′ end of *pbpB* (i.e., an intact TG domain and truncated TP domain) made the affected MRSA strain susceptible to β-lactams (31).

Proposed model of spermine–β-lactam synergy in *S. aureus*. Spermine was reported to exert a strong synergy effect with β-lactams on MRSA (20). In the current study, we present evidence that spermine alone also has a pH-dependent antibacterial activity against strains of *S. aureus* (MRSA and MSSA) and that this activity is most likely mediated by the nucleophilic property of spermine instead of its positive charges. In a search for the potential target of spermine by the genetic approach, the observed spermine-related phenotypes of MuM led us to propose that PBP 2 itself or enzymatic activities associated with the PBP 2-dependent complex in cell wall synthesis could be good candidates.

The working model we envisioned was as follows. Cell wall synthesis requires coordinated functions of a multienzyme complex to catalyze elongation of glycan chains and cross-linkage of peptide chains, and binding of spermine to this complex via PBP 2 elicits a conformational change to weaken interactions among enzymes in the complex and/or inhibit the TG activity of PBP 2. Given that a specific *pbpB* lesion confers resistance to spermine and spermine-oxacillin synergy to MuM, one would expect the TP domain of PBP 2 to be a potential target of spermine. However, we did not favor this hypothesis because TP-PBP 2 is not essential for growth of MRSA in the presence of PBP 2a. Moreover, the possibility of PBP 2a *per se* as target of spermine could also be excluded, because the spermine effects also exist in MSSA, in which PBP 2a is absent, and MuM possessing PBP 2a is resistant to spermine. Studies to elucidate the molecular mechanism for spermine effects based on the proposed model are currently in progress.

pH sensitivity of MuM. Because the TP domain of PBP 2 is truncated in MuM, it can grow in only a very limited pH range. The most striking difference between Mu50 and MuM in response to pH was under alkaline conditions (Fig. 4), which may be related to the cell wall turnover rate by the following rationale. It has been reported that the murein hydrolase exhibits a much lower level of activity under acidic conditions (38). Therefore, it is anticipated that alkaline conditions can speed up murein hydrolysis, which could have a more severe impact on MuM due to its weakened cell wall structure.

On the other hand, MuM also shows sensitivity to acidic pH. It is known that the transmembrane pH gradient is essential for the uptake of amino acids in *S. aureus* (24). The ability of MuM to adjust the transmembrane pH gradient may be reduced due to the PBP 2 mutation and concurrent cell wall anomaly, which could be a possible reason for its reduced growth rate when the pH is lower than 7. One explanation can be derived from the fact that PBP 2a is not detectable when growth is at pH 5.2 (13, 21), and therefore MuM without a functional TP of PBP 2 would encounter severe cell wall defects under acidic conditions.

In summary, several lines of evidence support PBP 2 as the potential target of spermine in sensitization of *S. aureus* to β-lactams. The absence of the TP domain in spermine-resistant MuM may liberate PBP 2 from spermine interference and concomitantly cooperate with PBP 2a to continue to be functional on exposure to β-lactams. The altered phenotypic properties and transcriptional adaptations could be the compensatory effects on cell wall composition triggered by mutated PBP 2. Future studies on the molecular mechanism of spermine interactions with the proposed PBP 2-associated multienzyme complex in cell wall synthesis hold great potential for the development of new therapeutics for MRSA infections.

ACKNOWLEDGMENTS

This work was supported in part by National Science Foundation grant NSF0950217 to C.-D. Lu and by a Molecular Basis of Disease Program fellowship from Georgia State University to X. Yao.

REFERENCES

1. **Andersson DI, Hughes D.** 2010. Antibiotic resistance and its cost: is it possible to reverse resistance? Nat. Rev. Microbiol. **8**:260–271.
2. **Antignac A, Sieradzki K, Tomasz A.** 2007. Perturbation of cell wall synthesis suppresses autolysis in *Staphylococcus aureus*: evidence for coregulation of cell wall synthetic and hydrolytic enzymes. J. Bacteriol. **189**: 7573–7580.
3. **Berger-Bächi B, Tschierske M.** 1998. Role of fem factors in methicillin resistance. Drug Resist. Updat. **1**:325–335.
4. **Bergeron RJ, et al.** 1995. The role of charge in polyamine analog recognition J. Med. Chem. **38**:2278–2285.
5. **Bore E, Langsrud S, Langsrud O, Rode TM, Holck A.** 2007. Acid-shock responses in Staphylococcus aureus investigated by global gene expression analysis. Microbiology **153**:2289–2303.
6. **Charpentier E, et al.** 2004. Novel cassette-based shuttle vector system for gram-positive bacteria. Appl. Environ. Microbiol. **70**:6076–6085.
7. **CLSI.** 2011. Performance standards for antimicrobial susceptibility testing. M100–S21; 21st informational supplement. Clinical and Laboratory Standards Institute, Wayne, PA.
8. **Cohen SS.** 1997. A guide to the polyamines. Oxford University Press, New York, NY.
9. **de Jonge BL, de Lencastre H, Tomasz A.** 1991. Suppression of autolysis and cell wall turnover in heterogeneous Tn*551* mutants of a methicillin-resistant *Staphylococcus aureus* strain. J. Bacteriol. **173**:1105–1110.
10. **de Jonge BLM, Chang YS, Xu N, Gage D.** 1996. Effect of exogenous glycine on peptidoglycan composition and resistance in a methicillin-resistant *Staphylococcus aureus* strain. Antimicrob. Agents Chemother. **40**: 1498–1503.
11. **Ghuysen JM.** 1991. Serine beta-lactamases and penicillin-binding proteins. Annu. Rev. Microbiol. **45**:37–67.
12. **Gurevitch J, Rozansky R, Weber D, Brzezinsky A, Eckerling B.** 1951. The role of spermine in the inhibition of Staphylococcus aureus by human semen. J. Clin. Pathol. **4**:360–365.
13. **Hartman BJ, Tomasz A.** 1984. Low-affinity penicillin-binding protein associated with beta-lactam resistance in *Staphylococcus aureus*. J. Bacteriol. **158**:513–516.
14. **Holtje J-V.** 1998. Growth of the stress-bearing and shape-maintaining murein sacculus of *Escherichia coli*. Microbiol. Mol. Biol. Rev. **62**:181–203.
15. **Höltje J-V.** 1996. A hypothetical holoenzyme involved in the replication of the murein sacculus of Escherichia coli. Microbiology **142**:1911–1918.
16. **Komatsuzawa H, et al.** 1997. Subcellular localization of the major autolysin, ATL and its processed proteins in Staphylococcus aureus. Microbiol. Immunol. **41**:469–479.

17. **Kuroda M, et al.** 2003. Two-component system VraSR positively modulates the regulation of cell-wall biosynthesis pathway in Staphylococcus aureus. Mol. Microbiol. **49**:807–821.
18. **Kuroda M, et al.** 2001. Whole genome sequencing of meticillin-resistant Staphylococcus aureus. Lancet **357**:1225–1240.
19. **Kuwahara-Arai K, Kondo N, Hori S, Tateda-Suzuki E, Hiramatsu K.** 1996. Suppression of methicillin resistance in a *mecA*-containing pre-methicillin-resistant *Staphylococcus aureus* strain is caused by the mecI-mediated repression of PBP 2′ production. Antimicrob. Agents Chemother. **40**:2680–2685.
20. **Kwon DH, Lu CD.** 2007. Polyamine effects on antibiotic susceptibility in bacteria. Antimicrob. Agents Chemother. **51**:2070–2077.
21. **Lemaire S, Fuda C, Van Bambeke F, Tulkens PM, Mobashery S.** 2008. Restoration of susceptibility of methicillin-resistant Staphylococcus aureus to beta-lactam antibiotics by acidic pH: role of penicillin-binding protein PBP 2a. J. Biol. Chem. **283**:12769–12776.
22. **Leski TA, Tomasz A.** 2005. Role of penicillin-binding protein 2 (PBP2) in the antibiotic susceptibility and cell wall cross-linking of *Staphylococcus aureus*: evidence for the cooperative functioning of PBP2, PBP4, and PBP2A. J. Bacteriol. **187**:1815–1824.
23. **Majerczyk CD, et al.** 2010. Direct targets of CodY in *Staphylococcus aureus*. J. Bacteriol. **192**:2861–2877.
24. **Niven DF, Hamilton WA.** 1974. Mechanisms of energy coupling to the transport of amino acids by Staphylococcus aureus. Eur. J. Biochem. **44**: 517–522.
25. **Oku Y, Kurokawa K, Ichihashi N, Sekimizu K.** 2004. Characterization of the Staphylococcus aureus mprF gene, involved in lysinylation of phosphatidylglycerol. Microbiology **150**:45–51.
26. **Palomo C, Oiarbide M.** 2010. β-Lactam ring opening: a useful entry to amino acids and relevant nitrogen-containing compounds, p 211–259. *In* Banik BK (ed), Heterocyclic scaffolds I, vol 22. Springer, Berlin, Germany.
27. **Pinho MG, de Lencastre H, Tomasz A.** 2001. An acquired and a native penicillin-binding protein cooperate in building the cell wall of drug-resistant staphylococci. Proc. Natl. Acad. Sci. U. S. A. **98**:10886–10891.
28. **Pinho MG, de Lencastre H, Tomasz A.** 1998. Transcriptional analysis of the *Staphylococcus aureus* penicillin binding protein 2 gene. J. Bacteriol. **180**:6077–6081.
29. **Pinho MG, Errington J.** 2005. Recruitment of penicillin-binding protein PBP2 to the division site of Staphylococcus aureus is dependent on its transpeptidation substrates. Mol. Microbiol. **55**:799–807.
30. **Pinho MG, Filipe SR, de Lencastre H, Tomasz A.** 2001. Complementation of the essential peptidoglycan transpeptidase function of penicillin-binding protein 2 (PBP2) by the drug resistance protein PBP2A in *Staphylococcus aureus*. J. Bacteriol. **183**:6525–6531.
31. **Pinho MG, Ludovice AM, Wu S, De Lencastre H.** 1997. Massive reduction in methicillin resistance by transposon inactivation of the normal PBP2 in a methicillin-resistant strain of Staphylococcus aureus. Microb. Drug Resist. **3**:409–413.
32. **Pohl K, et al.** 2009. CodY in *Staphylococcus aureus*: a regulatory link between metabolism and virulence gene expression. J. Bacteriol. **191**: 2953–2963.
33. **Pootoolal J, Neu J, Wright GD.** 2002. Glycopeptide antibiotic resistance. Annu. Rev. Pharmacol. Toxicol. **42**:381–408.
34. **Sauvage E, Kerff F, Terrak M, Ayala JA, Charlier P.** 2008. The penicillin-binding proteins: structure and role in peptidoglycan biosynthesis. FEMS Microbiol. Rev. **32**:234–258.
35. **Sobral RG, et al.** 2007. Extensive and genome-wide changes in the transcription profile of *Staphylococcus aureus* induced by modulating the transcription of the cell wall synthesis gene *murF*. J. Bacteriol. **189**:2376–2391.
36. **Sonenshein AL, Hoch JA, Losick R.** 2002. *Bacillus subtilis* and its closest relatives: from genes to cells. ASM Press, Washington, DC.
37. **Utaida S, et al.** 2003. Genome-wide transcriptional profiling of the response of Staphylococcus aureus to cell-wall-active antibiotics reveals a cell-wall-stress stimulon. Microbiology **149**:2719–2732.
38. **Yang SJ, Dunman PM, Projan SJ, Bayles KW.** 2006. Characterization of the Staphylococcus aureus CidR regulon: elucidation of a novel role for acetoin metabolism in cell death and lysis. Mol. Microbiol. **60**: 458–468.
39. **Zuniga M, Perez G, Gonzalez-Candelas F.** 2002. Evolution of arginine deiminase (ADI) pathway genes. Mol. Phylogenet Evol. **25**:429–444.